Applied Catalysis B: Environmental 121–122 (2012) 182–189

Contents lists available at SciVerse ScienceDirect

Applied Catalysis B: Environmental

journal homepage: www.elsevier.com/locate/apcatb

High efficiency of the cylindrical mesopores of MWCNTs for the catalytic wet peroxide oxidation of C.I. Reactive Red 241 dissolved in water

M. Soria-Sánchez[a], E. Castillejos-López[b], A. Maroto-Valiente[a], M.F.R. Pereira[c], J.J.M. Órfão[c], A. Guerrero-Ruiz[a,*]

[a] Dpto. Química Inorgánica y Técnica, Facultad de Ciencias, UNED, Unidad Asociada UNED-ICP/CSIC, P° Senda del Rey 9, 28040 Madrid, Spain
[b] Instituto de Catálisis y Petrol., CSIC, Campus Cantoblanco, 28049 Madrid, Spain
[c] Laboratório de Catálise e Materiais (LCM), Laboratório Associado LSRE/LCM, Faculdade de Engenharia, Universidade do Porto, 4200-465 Porto, Portugal

ARTICLE INFO

Article history:
Received 26 December 2011
Received in revised form 31 March 2012
Accepted 4 April 2012
Available online 11 April 2012

Keywords:
Carbon materials
Hydrogen peroxide
Adsorption
Catalytic decomposition

ABSTRACT

A study of the catalytic decolourisation of one textile dye by oxidation with H_2O_2, using different carbon materials as catalysts, is reported. Ten carbon solids, differing both in their texture–structure features and in their surface chemistry properties, were used for this purpose. These are two activated carbons, a high surface graphite, two structured nanomaterials (carbon nanofibres and carbon nanotubes), and the derivative samples prepared by oxidation of the pristines with nitric acid solutions. All these samples were characterised by determination of the nitrogen adsorption isotherms, thermogravimetric data, transmission electron microscopy, pH at the point of zero charge and chemical composition based on the X-ray photoelectron spectra. These carbon materials were evaluated as catalysts for the catalytic wet peroxide oxidation of C.I. Reactive Red 241 dissolved in water. Carbon nanotubes (CNTs) exhibit the highest performance in terms of activity for the catalytic wet peroxide oxidation, achieving a total removal of the dye after 90 min in process. It appears that catalytic activity for this reaction is improved by the internal cylindrical mesopores of CNTs. However, when these hydrophobic CNTs are treated by incorporation of oxygen surface groups which increase their hydrophilic character, the high catalytic performance of CNTs largely disappears.

1. Introduction

Activated carbons are conventional adsorbents which are commonly used in wastewater treatments for removing undesirable organic chemicals. The texture of these materials consists mainly of micropores (diameters < 2 nm), where the adsorption of large-sized solutes, such as dyes, pharmaceutical antibiotics, natural organic polyelectrolytes or alkylphenolic surfactants, might be markedly impeded by the size-exclusion effect. This type of steric effect, or the associated kinetic limitations of the adsorption of organic chemicals pollutants inside the micropores, can be largely prevented by exploring alternative mesoporous carbon adsorbents. For example, high surface graphites exhibit only opened surfaces, and therefore have high potential to act as adsorbents [1]. In the same line, carbon nanotubes (CNTs), especially multiwalled samples, have shown an improved adsorption capacity for organic compounds dissolved in water as well as for the desorption steps, compared with the typical microporous activated carbon adsorbents [2,3]. CNTs are composed of cylindrical mesopores formed with curved graphite sheets, and in general exhibit hydrophobic character. Furthermore, this cylindrical mesoporosity can enhance their adsorption properties [2]. In general, carbon material surfaces can be easily functionalised by oxidation treatments, leading to an enhancement, or decrease, of their adsorption efficiency as well as a modification of their catalytic properties. Also the interactions of organic molecules with the graphitic surfaces, functionalised or not (internal or external in the case of CNTs), can be tuned in order to improve the adsorption of organic compounds from water solutions [4]. Additionally, the aromatic rings of graphite sheets contain sp^2-hybridised carbon atoms with high electronic polarisability and hence may interact strongly with many aromatic compounds via π–π coupling/stacking. In relation to this, some reports argue the promising CNT properties for wastewater treatments [5,6]. For these applications it is required a deep understanding of the mechanisms and factors that control the organic compounds interactions over the carbon surface structures. However, studies on the interaction of organic chemicals dissolved in water over functionalised CNTs are still very scarce in the literature, white they are more abundant concerning their use as catalysts for some specific reactions [7] including methane decomposition, oxidative dehydrogenation, de-NOx reactions, selective oxidation of H_2S, esterification, hydroxylation and oxidation

* Corresponding author.
E-mail addresses: aguerrero@ccia.uned.es, aguerrero@icp.csic.es (A. Guerrero-Ruiz).

0926-3373/$ – see front matter © 2012 Elsevier B.V. All rights reserved.
http://dx.doi.org/10.1016/j.apcatb.2012.04.004

Table 1
Nomenclature of the materials.

Starting materials	Sample	Treatment
CNTs-N	CNTs-N	Ball-milled
	ox/CNTs-N	HNO_3 (6 M), reflux (3 h)
CNFs	CNFs	–
	ox/CNFs	HNO_3 (6 M), reflux (72 h)
HSAG	HSAG	–
	ox/HSAG	HNO_3 (concentrated), evaporation (348 K)
AC	AC	HCl (10 wt%), evaporation (65 °C)
	ox/AC	HNO_3 (6 M), reflux 72 h
NORIT	NORIT	–
	ox/NORIT	HNO_3 (6 M), reflux 3 h

processes [8,9]. It should be mentioned the potential applications of CNTs in the field of pollutant removing from waters, either as photocatalysts [10] or as support wet air oxidation catalysts [11].

In the case of catalytic wet peroxide oxidation processes, whilst activated carbons are known as catalysts for the decomposition of hydrogen peroxide [12–14], only a few studies have been carried out using graphenes or CNT materials [15,16]. The reaction mechanisms are not completely established and it seems that free radical species can act as intermediates [12–14,17]. The formation of these radicals would take place by an electron-transfer reaction, similar to the Fenton mechanism. The recombination of free radical species in the liquid phase and/or onto the activated carbon surface (ACS) will produce water and oxygen, the overall reaction being:

$$H_2O_2\,(ACS) \rightarrow H_2O + 1/2O_2$$

The main objective of this study was to systematically investigate the adsorption and catalytic properties of different types of carbon materials, when used in the catalytic wet peroxide oxidation of an organic dye substrate by H_2O_2. The comparison between the different surface features of these materials should allow us to determine the dependence of adsorption and oxidation catalytic properties on the specific morphologies or on the chemical species.

2. Experimental

2.1. Carbon materials

Five commercial carbon materials were comparatively studied: multiwall carbon nanotubes (CNTs-N) provided by Nanocyl™ (3100 Series, 95% purity), carbon nanofibres (CNFs) provided by Pyrograph (Applied Science, 98% purity), high surface area graphite (HSAG) provided by Timcal, and two activated carbons (AC and NORIT) provided by ICASA (Cordoba, Spain) and Norit (GAC 1240 plus, Amersfoort, Netherlands), respectively. Pristine CNTs-N and activated carbon NORIT were treated with HNO_3 (6 M) at reflux for 3 h under stirring, in order to introduce oxygenated surface groups. Before acid treatment, CNTs-N were segmented (1–10 μm) by ball-milling in order to open both ends. CNFs and AC were treated for 72 h at reflux with HNO_3 (6 M). Before this oxidation, AC was treated with HCl in order to remove most of the inorganic impurities. Finally, HSAG was stirred and heated at 65 °C with concentrated HNO_3 until almost all the liquid was evaporated, and this procedure was repeated three times. Then, all samples were filtered through a hot fritted glass funnel, and washed with distilled water until there was an absence of NO_3^- ions in solution and a stable pH value. The samples were then dried at 120 °C over 2 days, and finally crushed to a powder. Nomenclatures of pristine and oxidised materials are given in Table 1.

All the samples were characterised by N_2 adsorption at 77 K. The N_2 isotherms were obtained in an automatic Micromeritics ASAP 2010 volumetric system. The BET equation was applied to the N_2 isotherms to obtain the surface area values. Thermogravimetric analyses (TGA) were conducted under He flow in a SDT Q_{600} microbalance. The sample was placed in a ceramic holder and heated with a 10 °C/min ramp up to 1000 °C, followed by an isothermal treatment at that temperature for 30 min. The transmission electron microscopy (TEM) micrographs were acquired in a JOEL JEM microscope at 200 kV. X-ray photoelectron microscopy (XPS) analyses were performed with an ESCA-PROBE P (Omicron) spectrometer by using Mg-K radiation (1253.6 eV). To obtain the point of zero charge (pH_{pzc}), the electrophoretic mobility (μ) of the samples vs pH were measured in a Zeta Meter 3.0+ at 298 K. As $\chi a > 1$ (χ is the reciprocal of Debye length and a is the particle radius), the Smoluchowski equation $\mu = \varepsilon_T \varepsilon_0 \xi/\eta$ was applied to obtain the zeta potential (ξ). The amount of suspended sample used in each determination was approximately 100 mg/l. The pH was adjusted with HCl and NaOH. Suspensions were stabilised 24 h before measurements. Also, the inorganic impurities of the activated carbon Norit were analysed by carrying out an XRD diffractogram (ScanningSeifert XRD 3000 p diffractometer) of the carbon ashes (the sample was previously calcinated under air at 773 K).

2.2. Adsorption and catalytic tests

Organic dye C.I. Reactive Red 241 (commercial name Rifafix Red 3BN, Scheme 1) was provided by CITEVE and its solutions were performed in distillate water. The initial concentrations of dye were 200 ppm. The maximum molecular dimensions are 23.6 × 9.8 (Å × Å) [18]. This dye is in its anionic form in the entire pH range of our studies. Each adsorption curve was obtained by contacting 800 mg of carbon materials (particle size < 0.1 mm) with 370 mL of solution in a closed glass reactor under shaking at 400 rpm and isothermically at 25 °C. Aliquots were successively extracted at predetermined times and the liquid was separated by filtration. The concentration of the solution was determined with an UV/Vis absorption spectrophotometer (T60 UV/Vis Spectrophotometer of PG Instruments Limited). All measurements were made at the wavelengths corresponding to maximum absorbance of the hydrogen peroxide (λ_{max} = 400 nm) and the dye (λ_{max} = 542 nm), respectively. In the case of hydrogen peroxide previous complexation with titanyl sulphate has been used before UV/Vis determinations, which provides the yellow colour [19]. The initial concentration of hydrogen peroxide in the solutions was 1 M. Under similar experimental conditions the catalytic wet peroxide oxidation tests were performed. These experiments of adsorption and of catalytic oxidation were carried out on all the carbon samples. Also some control tests, in the absence of carbon materials, were carried out under the same conditions and in the same reactor. Finally it should be remarked that initial pH of the solutions, both for hydrogen peroxide decomposition or catalytic oxidation, was fixed close to a value of 3.5; this value approaches 6.0, depending on the progress in the hydrogen peroxide decomposition reaction. The adsorption experiments were conducted at an initial pH of 7.0.

3. Results and discussion

3.1. Characterisation of carbon materials

Table 2 summarises some of the textural characteristics of the different carbon materials as received.

The AC and NORIT samples are essentially microporous materials, with more than 75% of the total pore volume corresponding to micropores. On the contrary, CNTs-N is basically mesoporous, as revealed from the N_2 adsorption isotherm shapes (figures not shown for the sake of brevity). The slow increase in nitrogen uptakes at low and intermediate relative pressures suggests that

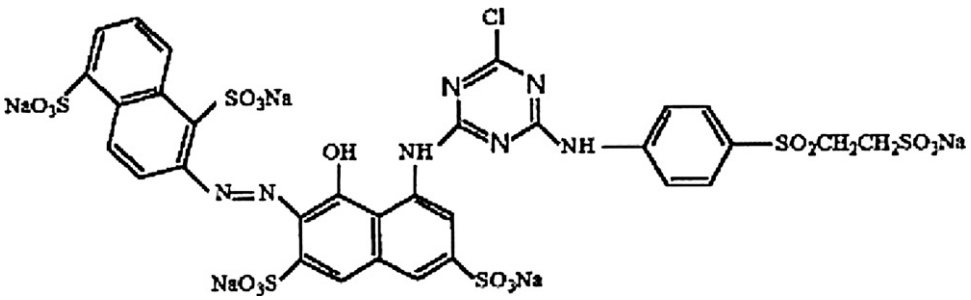

Scheme 1. Molecular structure of Rifafix Red 3BN.

the presence of micropores is negligible in CNT materials [20]. In the case of CNTs-N, at the medium relative pressure range (p/p_0 = 0.4–0.85) a hysteresis loop is clearly evidenced which is associated with condensation/evaporation in the inner hollow cavity of open ended CNTs [21]. Thus, a great fraction of CNTs have their end uncapped, as also revealed in the TEM micrographs (see SI1). Finally a sharp adsorption at high relative pressure, accompanied by hysteresis, indicates some capillary condensation within large mesopores [22], which are constituted by aggregated pores formed by interaction of isolated CNTs-N [23]. The small hysteresis loop in isotherms of samples indicates that there is a multilayer adsorption phenomenon as well as some restriction in the entrance of opening-up nanotubes. The central canal contributes to enhance the adsorbed amount at higher values of relative pressure. Finally CNFs exhibit external graphitic surfaces [24] with non-defined porosity and the HSAG sample has mesoporous texture [25].

Moreover Table 2 shows the point of zero charge (pH_{PZC}) values of the pristine samples. The as received activated carbon NORIT, in comparison with AC, presents a high value of pH_{PZC}. X-ray diffraction (XRD) and XPS of the carbon ashes showed the presence of impurities of silica and iron oxide on the untreated activated carbon NORIT (see SI2). In the case of the HSAG, AC and CNFs which have no surface inorganic impurities, the electrokinetic measurements show a low value of pH_{PZC}. The case of CNTs-N material gives place to neutral pH_{PZC} value. Table 2 also displays the oxygen content data estimated from the TG curves (see SI3). It is well known that CO_2 results from the decomposition of carboxyl, anhydride and lactonic groups, whereas CO results from phenolic, carbonyl, quinone, pyrone and anhydride groups [26]. As received CNT-N and NORIT samples present a small amount of surface oxygen functionalities (Table 2). This fact, together with the results obtained from pH_{PZC} (Table 2), indicates that the starting commercial activated carbon NORIT has a slightly basic nature. The concentration of oxygen surface groups in HSAG, CNFs and AC is higher pointing to the presence in some extension of oxygen groups on pristine surfaces.

Table 3 summarises the textural characteristics of the oxidised carbon materials. The HNO_3 treatment gives rise to a decrease of the apparent surface areas of HSAG, AC and NORIT materials and also produces a modification of the pore distribution. In this way, the oxidation causes the diminution in volume and the widening of the activated carbon micropores, giving rise to an increase in the mesopore volume. Also it is possible that part of the oxygen surface groups could block the entrance to the porous giving a decrease of the apparent surface areas [1]. In the case of CNTs, the apparent surface area of ox/CNTs-N increases, in comparison with the CNTs-N sample, suggesting that the acid treatment could remove some of the cups of tubes [27], which were not opened after the ball-milling process. Nitric acid treatment allows the introduction of polar hydrophilic surface groups such as —COOH groups and also phenol, carbonyl and quinones [28]. Thermogavimetric analyses (see SI3) performed under He provide a determination of the oxygen surface groups content (Table 3). As can be seen in this table, the nitric acid treatment introduces more oxygen surface groups per unit area on the HSAG surface than on the AC, NORIT, CNTs-N or CNFs. Thus, the density of oxygen groups on ox/HSAG surface is higher than on ox/AC, ox/NORIT, ox/CNTs-N and ox/CNFs. In the case of CNTs-N and NORIT samples, the duration of this treatment was limited to 3 h to avoid extensive internal surface functionalisation and/or the destruction and/or the widening of the micropores, respectively. CNFs and AC were functionalised with nitric acid for 72 h, pointing to a lower reactivity of the corresponding surfaces compared to others.

The surface/semi-quantitative analyses (XPS) (Table 4) confirm the functionalisation of the samples and the type of functional groups on the prepared samples. The relative amounts of the different elements, C and O, were calculated from the corresponding peak areas divided by the sensitivity factors (1.00 for C and 2.85 for O). The shapes of the high resolution C1s spectra for all samples (SI4-1) were similar to each other, with a predominant asymmetric peak, and a very small contribution of C in surface oxygen functional groups on the high energy side of the main peak. The deconvolution was carried out as described in [8,24]. The O/C ratios obtained for ox/CNFs suggest a moderate increase in the oxygen content for oxidised samples, which confirm the results obtained by TG. The activated carbon NORIT shows a more disordered structure with less developed graphene layers (Table 4). In the case of ox/CNTs-N and ox/NORIT, there is partial destruction of the graphitic structure or a lower delocalisation of the electrons since the relative concentration of C=C surface entries decreased, while the C—C ones increased. However, it is important to remark that our acid treatment only caused minimum textural damage to the samples (cf. Tables 3 and 4). The deconvolution of the O1s spectra (see SI4-2) is also used to obtain information on the nature of the surface oxygen groups. This peak can be deconvoluted into three components: oxygen in carbonyl and quinone groups (C=C, 531.4 eV); oxygen in hydroxyl and ether groups (C—O, 532.6 eV); and oxygen in acidic

Table 2
Textural and surface properties of the pristine samples.

Sample	BET (m^2/g)	Ash (%)	pH_{PZC}	μmol CO_2/m^2	μmol CO/m^2	CO/CO_2
CNTs-N	331	1.6	7.0	0.6	1.9	3.2
CNFs	30	3.7	4.5	1.4	10.7	7.4
HSAG	314	0.8	3.6	1.3	3.5	2.7
AC	1190	3.9	4.0	1.6	1.0	0.6
NORIT	972	4.6	8.5	0.2	0.9	4.0

Table 3
Textural and surface properties of the oxidised samples.

Sample	BET (m^2/g)	Ash (%)	μmol CO_2/m^2	μmol CO/m^2	CO/CO_2
ox/CNTs-N	476	0.0	1.6	4.5	2.8
ox/CNFs	38	1.6	2.1	11.8	5.7
ox/HSAG	111	0.4	5.5	12.7	2.3
ox/AC	711	0.8	2.7	8.3	3.1
ox/NORIT	909	0.9	0.8	2.4	3.1

carboxyl groups (COOH, 534.6 eV). SI4-2 displays the spectra for samples and in Table 4 the concentrations of the different species are presented. In general, acid treatments seem to introduce more carboxylic groups, although to a lower extent for the CNTs sample. In this instance the proportion of carbonylic groups introduced is higher.

3.2. Adsorption of the reactive dye

Kinetics of adsorption of the reactive dye at 25 °C were determined at a fixed pH value of 7 for all the carbon materials. As shown in Fig. 1, the adsorption capacity trend is: AC < CNFs < NORIT ~ HSAG < CNTs-N and in the case of the oxidised samples: ox/AC < ox/HSAG ~ ox/Norit < ox/CNFs < ox/CNTs-N.

When the solution pH is higher than the pH_{pzc}, the surface of the adsorbent is negatively charged, favouring the adsorption of cationic species, while for a solution with pH lower than the pH_{pzc} the surface is positively charged, favouring the adsorption of anionic species [29]. Considering the constant pH value of our solutions and the pH_{PZC} values of the pristine samples (Table 2), we can conclude that both the carbon surfaces and reactive dye species are charged negatively, with the exception of the NORIT sample, which should have a positively charged surface. Therefore, the results presented in Fig. 1 indicate that the adsorption of the dye should be caused mainly by weak dispersion forces [30], while electrostatic forces seem to not participate significantly. This interpretation is supported because the adsorption capacities obtained for the NORIT (positively charged surface) are similar to those determined for the HSAG (same adsorbed amount), which has a negatively charged surface (Fig. 1a). In addition, if the electrostatic forces were dominant in the adsorption mechanism, electrostatic repulsion between the anionic dye species and the HSAG surfaces will take place, which is not apparent according to our results. Hence, the adsorption of this reactive dye on pristine carbon materials can be due to the stacking interactions between the delocalised π electrons in the carbon basal planes and the free electrons in the dye molecules (aromatic rings and N=N bonds), in competition with the adsorption of water molecules. CNTs-N exhibits a hydrophobic surface, particularly in the inner cavity of the tubes, so strong π-stacking interactions between CNTs and the dye can be seen. This can also be an explanation to justify this adsorbent as the best for dye retention (Fig. 1c). It should be raised that the adsorption kinetic experiments were conducted at an initial pH value of around 7.0 in the solution; however in the catalytic wet peroxide oxidation tests the pH can reach values of 3.5. In order to verify if these pH variations can affect the adsorption kinetic curves obtained with the CNT sample, and indirectly if the dominant adsorption mechanism is through the π-stacking interactions, the adsorption kinetic curve at pH 3.5 over the CNT was recorded (see SI5). The adsorption values obtained are slightly lower than those obtained at pH 7 (Fig. 1), thus we can conclude that the dye adsorption cannot be related to the CNTs point of zero charge, avoiding the adsorption mechanism with ionic species.

In the case of activated carbons, NORIT or AC, their lower mesoporosity seem to be a limiting factor for the adsorption of the dye, revealing that pore sizes are critical for adsorption of relatively big molecules. In addition, pristine AC presents an important amount of functional groups, and they could block a large number of micropores, as well as modify the hydrophobic character, the amount of dye adsorbed being lower than in the case of NORIT. In general, pristine samples which have not been oxidised are those that present higher dye retention performances, while those that have been submitted to oxidation (presenting a large amount of oxygen surface groups) exhibit lower adsorption capacities. Thus oxygenated groups seem to act as hydrophilic centres [31], and water molecules can form H-bond with these functional groups, which will either compete with the dye for adsorption sites [32] or form three-dimensional clusters blocking the adsorption sites nearby [33]. In short, the H-bond formation between water molecules and superficial oxygen functional groups acts by effectively decreasing the adsorption of the dye. It is also possible that the presence of oxygenated groups could block [4,34,35] access to the inner cavity in the case of CNT samples [36].

3.3. Catalytic decomposition of hydrogen peroxide

Fig. 2 shows the evolution of H_2O_2 concentrations upon time with all the samples. These experiments are critical to differentiate the effect of the carbon chemical surface properties on the decolourisation, both promoting the catalytic oxidation or just by adsorption. The hydrogen peroxide decomposition was

Table 4
XPS atomic ratios and relative content of carbon and oxygen-containing functional groups determined from the C1s and O1s region for the different samples.

Samples	C1s (wt%)						O/C	O1s (wt%)		
	C=C	C—C	C—O	C=O	COO	C[a]		C—O	C=O	COOH
AC	78.5	2.5	7.9	5.9	2.2	3.1	0.150	41.8	44.1	14.1
ox/AC	72.5	2.7	13.6	3.0	4.2	4.1	0.255	48.9	13.0	38.0
NORIT	88.8	6.5	2.2	1.0	0.70	0.68	0.041	49.7	29.2	21.1
ox/NORIT	74.6	7.1	7.4	6.0	4.1	0.81	0.166	37.8	30.5	31.8
HSAG	88.8	1.4	1.2	0.87	0.32	7.4	0.018	45.9	40.2	13.9
ox/HSAG	88.3	2.2	1.8	2.0	0.61	5.1	0.039	33.1	41.4	25.8
CNFs	93.1	0.5	0.54	0.24	0.18	5.5	0.010	48.9	21.1	29.9
ox/CNFs	90.5	0.98	0.75	0.48	0.43	6.8	0.017	37.1	23.6	39.4
CNTs-N	91.30	0.73	0.63	0.44	0.15	6.74	0.008	45.6	33.3	21.1
ox/CNTs-N	81.77	3.22	3.63	2.84	0.96	7.58	0.057	35.2	54.6	10.3

[a] π–π shake-up peak contributions.

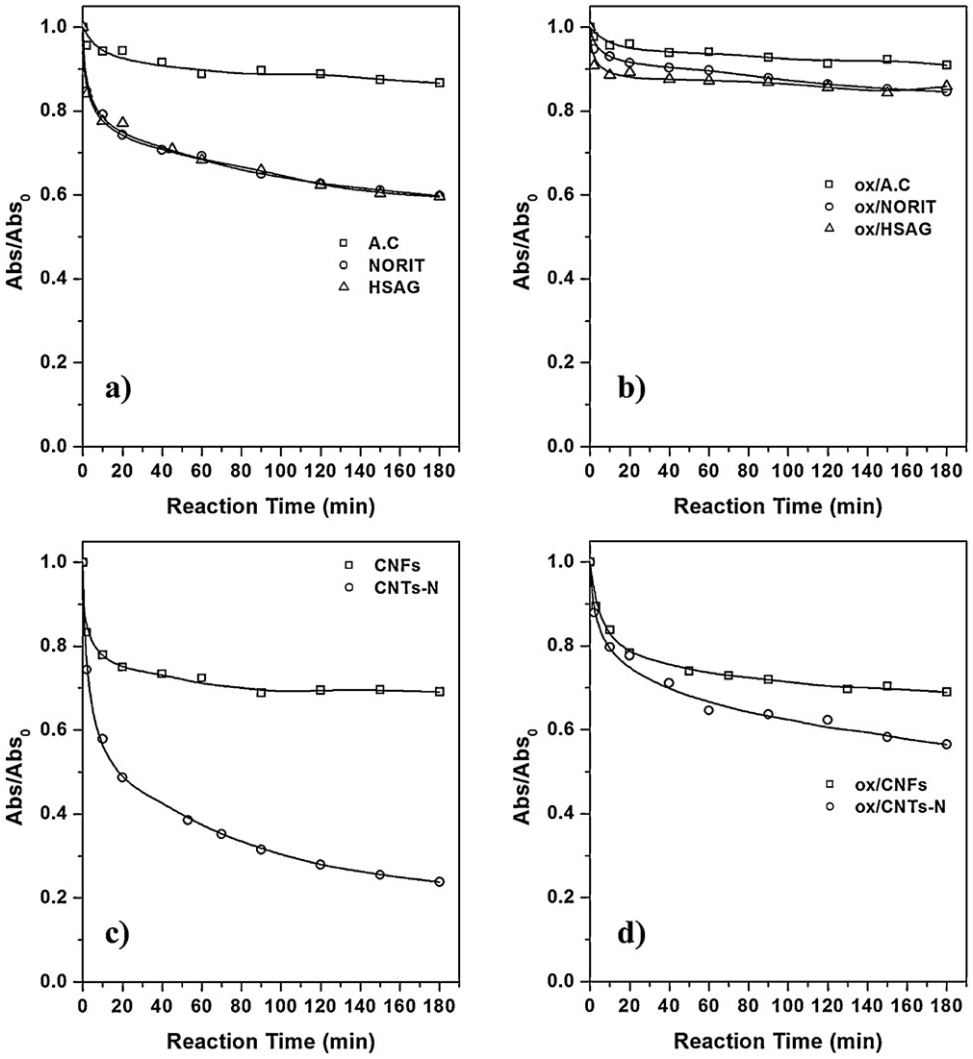

Fig. 1. Adsorption kinetics of reactive dye (initial concentration 200 ppm) at 25 °C on: (a) AC, NORIT, HSAG, (b) ox/AC, ox/NORIT, ox/HSAG, (c) CNFs, CNTs-N and (d) ox/CNFs, ox/CNTs-N. The initial pH of the solution was 7.0.

determined at the pH of the H_2O_2 solution (pH = 3.5). This indicated that almost all samples were positively charged, except HSAG, the surface of which exhibits an almost neutral charge. Fig. 2 shows that the decomposition of H_2O_2 in the absence of carbon samples (blind test) is not significant. In general, NORIT activated carbon yielded the highest catalytic activities being capable of decomposing hydrogen peroxide at 100% in 1.5 h under our experimental conditions (Fig. 2a). In order to understand the behaviour of activated carbon NORIT we have to use the previous reported characterisation data. NORIT sample presents the most disordered structures and microcrystallites contain few graphene layers (see XPS results), exposing at its surface a large concentration of electron-rich active sites, which could be capable of decomposing hydrogen peroxide according to the electron-transfer mechanism. In addition, the micropore entrances may be regions with more sites of this type and the texture is highly governed by microporosity. However, the AC sample exhibits similar structural ordering than that found in the NORIT activated carbon, but its decomposition capacity is much lower (Fig. 2a). The different catalytic efficiencies to decompose H_2O_2 detected for the two activated carbons, NORIT and AC, suggests that: (1) the slightly basic nature or the inorganic impurities on NORIT could improve the H_2O_2 decomposition and/or (2) the hydrogen peroxide decomposition rate decreases in the presence of surface oxygen groups.

Concerning the inorganic impurities present on the untreated activated carbon NORIT, these were mainly detected in the ashes; and they were analysed by XRD and XPS (see SI2), and quantitatively determined gravimetrically (see Tables 2 and 3), we can state that iron species are present in the case of NORIT activated carbon (not in the case of AC sample) together with SiO_2, and these impurities can be responsible for the H_2O_2 decomposition. On the other hand, the presence of surface oxygen groups could reduce the concentration and reactivity of the unsaturated carbon active sites, because the surface oxygen groups are precisely generated on the most active carbon sites during the oxidation treatment, thus decreasing the available catalytic sites for the H_2O_2 decomposition. However, when the oxidation treatment to incorporate oxygen surface groups is carried out, with a highly concentrated nitric acid solution, we are effectively removing the iron inorganic impurities (see Table 3). Finally the comparison of AC and ox/AC (or CNTs-N and ox/CNTs-N) samples indicated that the presence or absence of oxygen surface groups is not a critical parameter for the H_2O_2 decomposition, although some influence may exist.

3.4. Catalytic decomposition of the reactive dye Rifafix Red 3BN

Fig. 3 shows comparatively the dye decolourisation performance of carbon materials either by adsorption or by catalytic wet

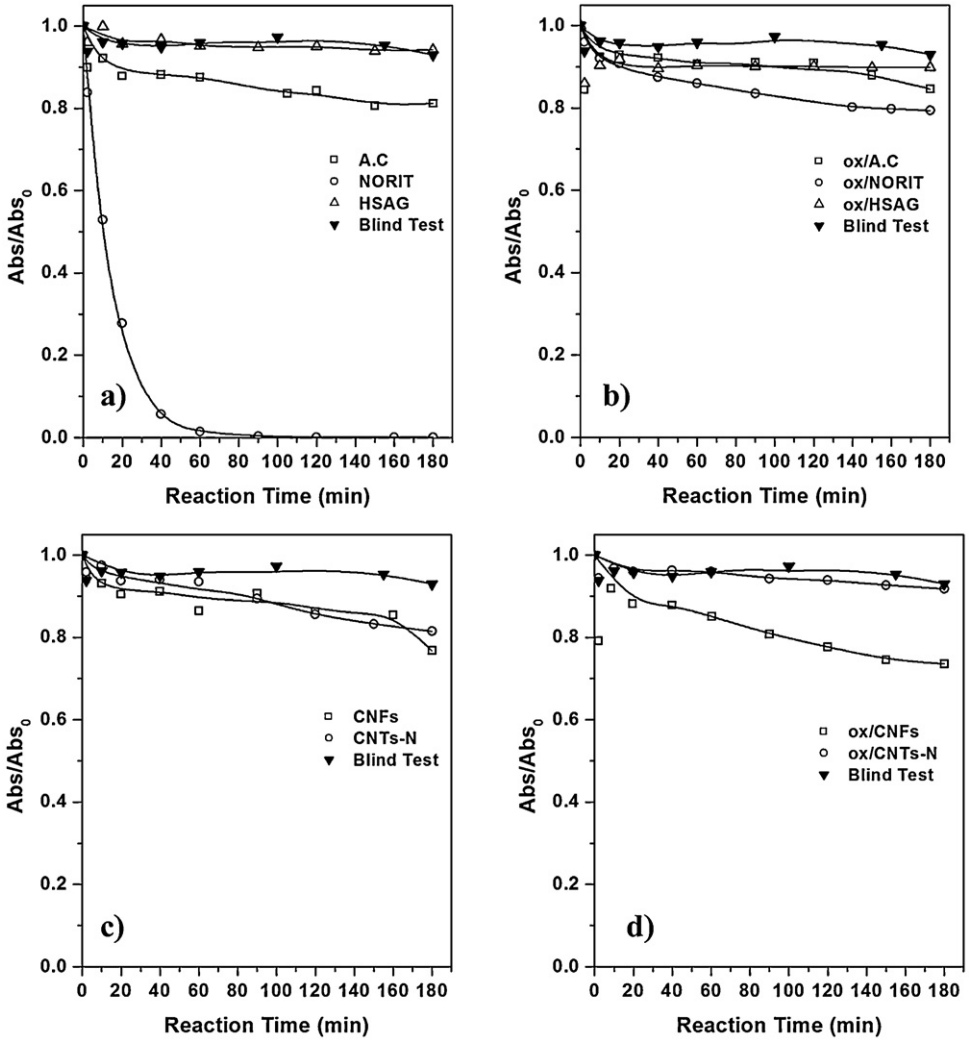

Fig. 2. Hydrogen peroxide decomposition (initial concentration 1 M and pH 3.5) on: (a) AC, NORIT, HSAG, (b) ox/AC, ox/NORIT, ox/HSAG, (c) CNFs, CNTs-N and (d) ox/CNFs, ox/CNTs-N.

peroxide oxidation. The catalytic wet peroxide oxidation data in the presence of activated carbons, AC or NORIT, reveals low catalytic activities for colour removal since the values obtained by adsorption are close to those measured in catalytic wet peroxide oxidation. Hence, the dye C.I. Reactive Red 241, which was efficiently removed by adsorption on the NORIT activated carbon, cannot be oxidised by H_2O_2. Nevertheless, this carbon is the only one providing a total H_2O_2 decomposition (Fig. 2); thus the present results suggest that this material seems to promote the decomposition of H_2O_2 to •OH radicals (mechanism based on iron species) but is unable to perform the catalytic oxidation. In general, activated carbons do not exhibit significant catalytic activity for decolourisation, and the removal of dyes is achieved just by adsorption. The same behaviour has been detected for oxidised activated carbons, ox/AC and ox/NORIT samples (Fig. 3b), both exhibiting low catalytic activities. On the opposite, in the case of HSAG, showing a substantially less efficient H_2O_2 decomposition activity compared with NORIT, the produced •OH radicals (small amounts but generated only on the carbon surface where the dye is adsorbed) a significant catalytic effect can be observed. So, the colour removal after 180 min increases, passing from 41% in the adsorption process to 55% during the catalytic wet peroxide oxidation of the dye.

In the above reasoning we are assuming that the hydroxyl radicals are very active in the oxidation of organic substrates in the aqueous phase [37], and that HSAG carbon not only catalyses the decomposition of H_2O_2. Also carbons can act generating some active free radicals, over surface sites exposed on the edges or steps of the graphitic structures (which have capacities for the H_2O_2 decomposition reaction). These surface sites can cooperatively participate in the adsorption of the dye molecules, improving the catalytic wet peroxide oxidation activity, and finally modifying some of the Fenton reaction pathways [12]. In relation to the oxidised sample, ox/HSAG, the presence of electron-withdrawing oxygenated groups on the carbon surface of this material seems not to be favourable for the dye adsorption processes nor for the catalytic wet peroxide oxidation reaction as this graphite does not present any significant catalytic activity. Similar arguments can be applied for the carbon nanofibres (CNFs and ox/CNFs samples) as shown in Fig. 3c and d.

In contrast, our results show that the highest catalytic activity corresponds to the sample that lead to the highest adsorption dye capacity, i.e. sample CNTs-N. Values of catalytic oxidation are close to 100% decolourisation after 90 min in the reaction on this sample. However, at this point, the dyes selective adsorption removed around 70% of the dye, and so the catalytic wet peroxide oxidation remarkably increases the elimination of C.I. Reactive Red by an additional 30%. Also this effect is faster than on the other carbon materials. Thus, the special morphology, composed of cylindrical

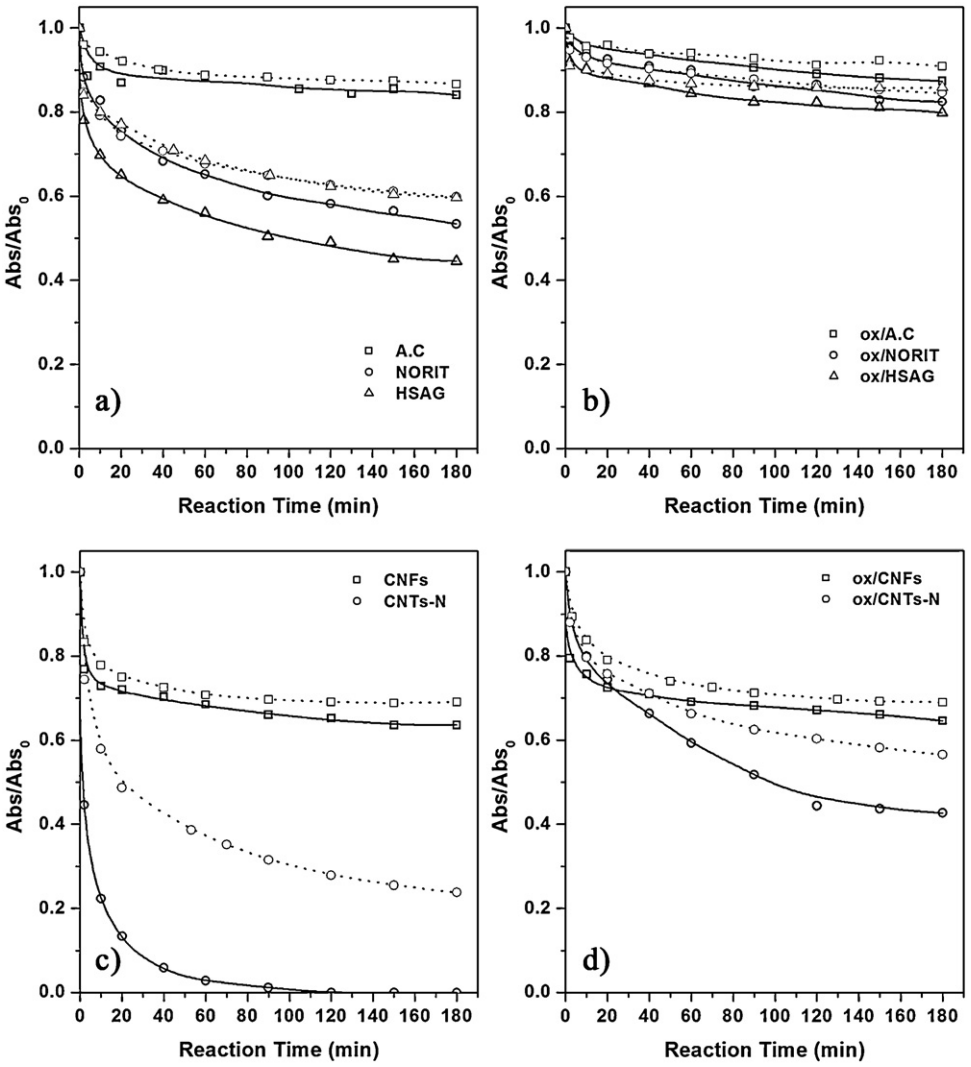

Fig. 3. Catalytic oxidation by hydrogen peroxide (solid line, where are combined adsorption and degradation) and adsorption of the dye (pointed line) using the different carbon materials: (a) AC, NORIT, HSAG, (b) ox/AC, ox/NORIT, ox/HSAG, (c) CNFs, CNTs-N and (d) ox/CNFs, ox/CNTs-N. Initial concentration of H_2O_2 1 M and of dye C.I. Reactive Red 200 ppm.

mesopores formed with curved graphite sheets and the surface chemistry of the CNTs-N material should play a critical role in its efficiency during the catalytic wet peroxide oxidation reaction, probably promoting the decomposition of H_2O_2 with formation of •OH radicals inside the mesopores. In spite of the short life of •OH radicals, the cylindrical mesopores of the CNTs allow them to react with the adsorbed dye in direct proximity. Then, among the possible regions for the reaction between generated •OH radicals and the dye, the internal cylindrical pores of CNTs could permit, by confinement effects, the fast and direct contact between those radicals and the substrate preventing the loss of active radicals just on unsaturated carbon surface sites. Several theoretical studies have shown that catalysed chemical reactions can be influenced by confinements due to its correlation with the collision theory of chemical reactions, the significantly reduced reaction volume, and the interaction of reactants and products with the internal channel of CNTs [38,39] must be considered in this line. For instance, Santiso et al. [40] showed from theoretical studies that the shape catalytic effect can be even more important than chemical interaction effects when adsorbed species react. These authors explained that kinetics of reactions can be radically altered, with rate modifications of many orders of magnitude, when narrow pores are presented. Another special property of the CNTs-N sample is its hydrophobic character. When oxygen surface groups are incorporated on the surface of this material yielding ox/CNTs-N, both the dye adsorption capacity and the catalytic wet peroxide oxidation activity are strongly reduced. The reduction in the dye decomposition rate observed, in general, on the oxidised samples (Fig. 3) can be attributed to the reduction of catalytically active surface sites (occupied by water molecules, preferentially adsorbed over more hydrophilic surfaces), which become unavailable for the activation of H_2O_2 or for the dye adsorption. Furthermore, in the case of the oxCNTs-N sample, the oxygen surface groups can also block the access to the inner mesopores of CNTs, then reducing the adsorption capacity (see Fig. 1).

4. Conclusions

The surface chemistry of carbon materials plays a significant role in the adsorption process of the C.I. Reactive Red from aqueous solutions. The presence of oxygenated groups on all carbon materials is unfavourable to the dye adsorption. The oxygen groups also reduce the concentration and reactivity of the unsaturated surface carbons, which are required active sites for the H_2O_2 decomposition, where hydroxyl radicals are generated. In the case of activated carbon, the presence of inorganic impurities give place to an improved

decomposition of H_2O_2 but this fact is not relevant from the point of view of the catalytic wet peroxide oxidation reaction. Thus sample HSAG, which only contains a limited amount of oxygenated surface groups, is more efficient as a catalyst than the studied activated carbons, in spite of its lower surface area (three to four times less).

Remarkably, pristine CNTs (sample CNTs-N) are the best adsorbent for the dye and the more efficient catalyst for the catalytic wet peroxide oxidation reaction and total removal of the C.I. Reactive Red after 90 min at room temperature being observed under our experimental conditions. Thus, by a judicious selection of a carbon material, where confinement effects in the inner cavity of CNTs can take place, it emerges an improved oxidation catalyst for removing dye from wastewater using a catalytic wet peroxide oxidation reaction. Finally, our results clearly identify that confinement effects inside CNTs can be useful for wastewater depollution treatments.

Acknowledgements

M. S. gratefully acknowledges a predoctoral grant from the UNED. This work was carried out with the support of Fundação para a Ciência e a Tecnologia (FCT), Portugal and FEDER, in the context of Programme COMPETE under project NANO/NTec-CA/0122/2007 and of the Spanish MICINN under projects CTQ2011-29272-C04-01 and -03, EUI2008-205 and -185.

Appendix A. Supplementary data

Supplementary data associated with this article can be found, in the online version, at http://dx.doi.org/10.1016/j.apcatb.2012.04.004.

References

[1] D.M. Nevskaia, E. Castillejos-López, V. Muñoz, A. Guerrero-Ruíz, Carbon 42 (2004) 653–665.
[2] B. Pan, B. Xing, Environmental Science and Technology 42 (2008) 9005–9013.
[3] Y. Kun, X. Baoshan, Environmental Pollution 145 (2007) 529–537.
[4] D. Nevskaia, E. Castillejos-Lopez, V. Muñoz, A. Guerrero-Ruiz, Environmental Science and Technology 38 (2004) 5786–5796.
[5] D. Tasis, N. Tagmatarchis, A. Bianco, M. Prato, Chemical Reviews 106 (2006) 1105–1136.
[6] T. Masciangioli, W.X. Zhang, Environmental Science and Technology 37 (2003) 102–108.
[7] P. Serp, in: P. Serp, J.L. Figueiredo (Eds.), Carbon Materials for Catalysis, vol. 9, J. Wiley & Sons, Hoboken, NJ, 2009, pp. 309–372.
[8] M. Soria-Sánchez, A. Maroto-Valiente, J. Álvarez-Rodríguez, V. Muñoz-Andrés, I. Rodríguez-Ramos, A. Guerrero-Ruíz., Applied Catalysis B: Environmental 104 (2011) 101–109.
[9] A.G. Gonçalves, J.L. Figueiredo, J.J.M. Orfao, M.F.R. Pereira, Carbon 48 (2010) 4369–4381.
[10] C. Martinez, L.M. Candle, M.I. Fernandez, J.A. Santaballa, J. Faria, Applied Catalysis B: Environmental 107 (2011) 110–118.
[11] F.J. Benitez, J. Garcia, J.L. Acero, F.J. Real, G. Roldan, Process Safety and Environment Protection 89 (2011) 334–341.
[12] A. Georgi, F.D. Kopinke, Applied Catalysis B: Environmental 58 (2005) 9–18.
[13] L.B. Khalil, B.S. Girgis, T.A. Tawfik., Journal of Chemical Technology and Biotechnology 76 (2001) 1132–1140.
[14] H. Huang, M. Lu, J. Chen, C. Lee, Chemosphere 51 (2003) 935–943.
[15] F. Lucking, H. Koser, M. Jank, A. Ritter, Water Research 32 (1998) 2607–2614.
[16] X. Hua, B. Liu, Y. Deng, H. Chen, S. Luo, C. Sun, P. Yang, S. Yang, Applied Catalysis B: Environmental 107 (2011) 274–283.
[17] H. Huang, M. Lu, J. Chen, C. Lee, Chemosphere 51 (2003) 935–941.
[18] J.L. Figueiredo, J.P.S. Sousa, C.A. Orge, M.F.R. Pereira, J.J.M. Orfao, Adsorption 17 (2011) 431–441.
[19] M.F.R. Pereira, S.F. Soares, J.J.M. Órfao, J.L. Figueiredo, Carbon 41 (2003) 811–821.
[20] M. Eswaramoorthy, C. Rahul Sen, N.R. Rao, Chemical Physics Letters 304 (1999) 207–210.
[21] Q.-H. Yang, P.-X. Hou, S. Bai, M.-Z. Wang, H.-M. Cheng, Chemical Physics Letters 345 (2001) 18–24.
[22] S.J. Gregg, K.S.W. Sing, Adsorption, Surface Area and Porosity, Academic Press, New York, 1982.
[23] E. Castillejos, P. Serp, in: D.M. Guldi, N. Martín (Eds.), Carbon Nanotubes and Related Structures: Synthesis, Characterization, Functionalization, and Applications, Chapter 11, Wiley-VCH Verlag GmbH & Co. KGaA, Weinheim, Germany, 2010, pp. 321–348.
[24] A.B. Dongil, B. Bachiller-Baeza, A. Guerrero-Ruiz, I. Rodríguez-Ramos, A. Martínez-Alonso, J.M.D. Tascón, Journal of Colloid and Interface Science 335 (2011) 179–189.
[25] E. Castillejos-López, B. Bachiller-Baeza, D.M. Nevskaia, V. Muñoz, I. Rodriguez-Ramos, A. Guerrero-Ruíz, Carbon 44 (2006) 3130–3133.
[26] K. Kinoshita, Carbon: Electrochemical and Physicochemical Properties, Wiley, New York, 1988.
[27] C. Wang, S. Guo, X. Pan, W. Chen, X. Bao, Journal of Materials Chemistry 18 (2008) 5782–5786.
[28] I. Gerber, M. Oubenali, R. Bacsa, J. Durand, A. Gonçalves, M. Fernando, R. Pereira, F. Jolibois, L. Perrin, R. Poteau, P. Serp, Chemistry - A European Journal 41 (2011) 11354–11477.
[29] L.R. Radovic, F. Rodríguez-Reinoso, in: P.A. Thrower (Ed.), Chemistry and Physics of Carbon, vol. 25, Dekker, New York, 1997, pp. 243–358.
[30] L.R. Radovic, C. Moreno-Castilla, J. Rivera-Utrilla, Chemistry and Physics of Carbon 27 (2000) 227–405.
[31] J.J.M. Órfão, A.I.M. Silva, J.C.V. Pereira, S.A. Barata, I.M. Fonseca, P.C.C. Faria, M.F.R. Pereira, Journal of Colloid and Interface Science 296 (2006) 480–489.
[32] F. Ahnert, H.A. Arafat, N.G. Pinto, Adsorption 9 (2003) 311–319.
[33] C.O. Ania, B. Cabal, C. Pevida, A. Arenillas, J.B. Parra, F. Rubiera, J.J. Pis, Applied Surface Science 253 (2007) 5741–5746.
[34] J.L. Figueiredo, M.F.R. Pereira, M.M.A. Freitas, J.J.M. Órfao, Carbon 37 (1999) 1379–1389.
[35] V.P. Santos, M.F.R. Pereira, P.C.C. Faria, J.J.M. Órfao, Journal of Hazardous Materials 162 (2009) 736–742.
[36] K. Yang, L.Z. Zhu, B.S. Xing, Environmental Science and Technology 40 (2006) 1855–1861.
[37] E. Neyens, J. Baeyens, Journal of Hazardous Materials 98 (2003) 33–50.
[38] P. Serp, E. Castillejos, Chemcatchem 2 (2010) 41–47.
[39] P. Xiulian, B. Xinhe, Accounts of Chemical Research 44 (2011) 553–562.
[40] E.E. Santiso, M.K. Kostov, A.M. George, M. Buongiorno Nardelli, K.E. Gubbins, Applied Surface Science 253 (2007) 5570–5579.